

Influence of microstructure on the thermal conductivity of magnetoresistive $\text{La}_{0.7}\text{Ca}_{0.3}\text{MnO}_3/\text{Mn}_3\text{O}_4$ manganite/insulating oxide polycrystalline bulk composites

J. Mucha,^{1,2,a)} B. Vertruyen,² H. Misiorek,¹ M. Ausloos,² K. Durczewski,¹ and Ph. Vanderbemden²

¹*W Trzebiatowski Institute for Low Temperature and Structure Research, Polish Academy of Sciences, P.O. Box 1410, 50-950 Wrocław 2, Poland*

²*Departments of Electrical Engineering & Computer Science (B28), Chemistry (B6), and Physics (B5), SUPRATECS, University of Liège, Sart-Tilman, B-4000 Liège, Belgium*

(Received 14 October 2008; accepted 31 December 2008; published online 17 March 2009)

We report the temperature dependence of the thermal conductivity $\kappa(T)$ of bulk polycrystalline composite samples containing a magnetoresistive manganite ($\text{La}_{0.7}\text{Ca}_{0.3}\text{MnO}_3$) and an electrically insulating phase (Mn_3O_4). The sample porosity is shown to be a significant parameter affecting the experimental data: after porosity correction the curves display the characteristics of an ideal composite. A fit of the $\kappa(T)$ curves at low temperature using the Debye model enables the mean free path of phonons scattered on “boundaries” to be determined. The values are on the order of the grain size but are influenced by the grain arrangement and the presence of twins. © 2009 American Institute of Physics. [DOI: 10.1063/1.3078796]

I. INTRODUCTION

The colossal magnetoresistance (CMR) of some $\text{La}_{1-x}\text{A}_x\text{MnO}_3$ compounds (where A is an alkaline earth) has attracted considerable research interest.^{1–4} In addition to the intrinsic MR effect, polycrystalline samples display an extrinsic MR effect due to the presence of grain boundaries.^{3–6} Several groups^{7,8} have shown that the extrinsic MR is enhanced by preparing composites of a magnetoresistive manganite and an insulating secondary phase. The insulating phase acts as an additional barrier to the conduction at the grain boundaries and increases the percolating conduction path. In our previous work,⁹ we have shown that well-sintered $\text{La}_{0.7}\text{Ca}_{0.3}\text{MnO}_3$ (LCMO)/ Mn_3O_4 composite samples can be obtained with almost constant manganite composition throughout the series. We have analyzed both (i) the dependence of the electrical conductivity as a function of the volume fraction of LCMO manganite phase¹⁰ and (ii) the unusual magnetoresistive properties.¹¹ In this paper we concentrate on the thermal conductivity properties of such composites and analyze the influence of phonon scattering on interfaces.

II. PREPARATION OF SAMPLES AND THEIR STRUCTURE

Bulk, dense LCMO/ Mn_3O_4 composite samples were prepared by spray drying.⁹ The composition of the phases was ascertained by x-ray diffraction and energy dispersive x-ray analysis.^{9,10} Five samples are considered in the present study: S1 is pure LCMO, S5 is pure Mn_3O_4 , and samples S2–S4 are composites of both phases. Scanning electron microscopy (Philips XL30 Field Emission Gun–Environmental Scanning Electron Microscope) (Ref. 10) revealed three

types of microstructures as the Mn_3O_4 content increases: (i) Mn_3O_4 islands in a LCMO matrix, (ii) a labyrinthine pattern of the two phases, and (iii) LCMO islands in a Mn_3O_4 matrix. The mean grain size lies in the range of 1–10 μm . Micrographs of fractured cross sections (Fig. 1) put into evidence changes in surface structure with increasing Mn_3O_4 content, with twins¹² clearly visible in Mn_3O_4 [Fig. 1(c)]. In addition, all samples exhibit some porosity. The dimensionless volume fractions of each phase, together with the pore volume fraction,¹⁰ are shown in Table I.

III. METHOD OF THERMAL CONDUCTIVITY MEASUREMENT AND ITS RESULTS

The thermal conductivity was measured using the stationary heat flux method in the temperature range of 5–300 K.^{13,14} The temperature difference along the sample was in the range of 0.1–0.5 K. Particular care was taken to avoid a parasitic heat transfer between the sample and its environment. The typical measurement error is below 2%, and the surplus error estimated from the scatter in the measurement points does not exceed 0.3%.

The temperature dependence of the thermal conductivity $\kappa(T)$ measured on the LCMO/ Mn_3O_4 composite samples is shown in Fig. 2(a), together with the thermal conductivities of pure LCMO (S1) and pure Mn_3O_4 (S5). These $\kappa(T)$ data need to be compared to magnetic phase transition temperatures: Mn_3O_4 exhibits a ferrimagnetic-paramagnetic transition at ~ 42 K,¹⁵ whereas the LCMO phase exhibits a ferromagnetic-paramagnetic transition at some Curie temperature T_C around 250 K, depending on the exact stoichiometry. The Curie temperatures of the LCMO phase in the different samples, determined from magnetic measurements,¹¹ are indicated by arrows in Fig. 2(a) and listed in Table I. For samples containing LCMO (S1–S4), a change in slope occurs at the Curie temperature of the

^{a)}Electronic mail: j.mucha@int.pan.wroc.pl.

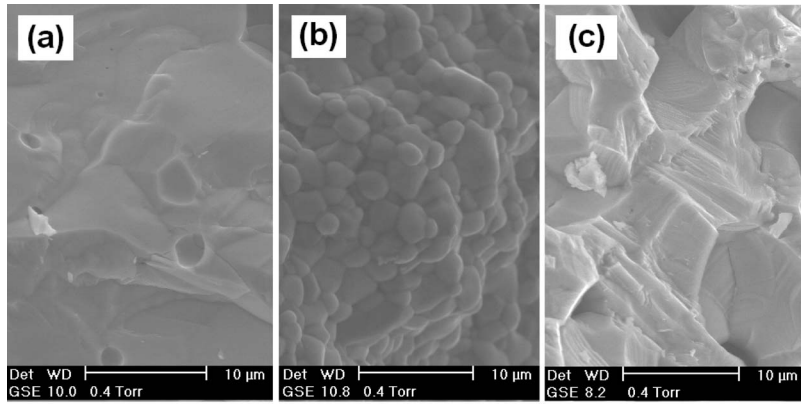


FIG. 1. Scanning electron microscopy pictures of fractured cross sections of samples (a) S1 (pure LCMO), (b) S3 (composite), and (c) S5 (pure Mn_3O_4).

LCMO phase. Such behavior is similar to that observed on pure CMR materials and is a consequence of the vanishing magnetic order above T_C .^{3,16–18} For samples containing a significant amount of Mn_3O_4 (S3–S5), a second glitch is observable at 42 K. The clear correlation between the magnetic phase transition temperatures and the thermal conductivity anomalies (as small as 0.05 W/m K) underlines the low scatter of the measurements.

IV. INTERPRETATION OF RESULTS

Next we turn to the magnitude of the thermal conductivity. Although the electrical conductivity of samples S1–S5 spans more than ten orders of magnitude,¹¹ the thermal conductivities of all samples are close to each other. Since the ceramic samples are slightly porous (cf. Table I), we correct the $\kappa(T)$ data displayed in Fig. 1 for porosity using the Maxwell model.¹⁹ In a host medium (thermal conductivity κ_0) containing randomly distributed and randomly sized spherical pores (volume fraction f), the effective thermal conductivity κ_{eff} of the sample (matrix+pores) is given by^{19–21}

$$\kappa_{\text{eff}} = \kappa_0 \frac{1-f}{1+f/2}. \quad (1)$$

The porosity correction consists of multiplying the measured $\kappa_{\text{eff}}(T)$ data by the factor $(1+f/2)/(1-f)$. The resulting values—i.e., the $\kappa_0(T)$ data that would be obtained in a 100% dense material—are plotted in Fig. 2(b). A log-log scale is used in order to better show the fitted curves (dashed lines) described in the paragraph below. Remarkably, after the porosity correction, all curves almost cross each other at $T^* \sim 70$ K. Physically, a crossing point shows that at the tem-

TABLE I. The volume fraction of each phase, together with the pore volume fraction measured by Archimedes's method. The last column shows the Curie temperature T_C of the LCMO phase.

Sample	LCMO volume fraction (%)	Mn_3O_4 volume fraction (%)	Pore volume fraction (%)	T_C (K)
S1	89	0	11	258
S2	91	4	5	256
S3	55	44	2	251
S4	12	66	22	217
S5	0	79	21	...

perature T^* where the two separate phases (LCMO and Mn_3O_4) have the same thermal conductivity κ^* , all composites of the two phases are also characterized by a thermal conductivity κ^* . In our composites, the real distribution and shape of the pores may differ from those assumed in Eq. (1), and a perfect crossing is not expected. The deviation from this ideal behavior, however, is surprisingly small and underlines the importance of the porosity correction.

Now we analyze the low-temperature behavior of the thermal conductivity, which can be considered as the sum of the contributions carried by phonons (κ_{ph}), conduction electrons (κ_e), and magnons (κ_{magn}), i.e., $\kappa = \kappa_{\text{ph}} + \kappa_e + \kappa_{\text{magn}}$.²² The temperature dependence of the electronic thermal conductivity $\kappa_e(T)$ was estimated by assuming the validity of the Wiedemann–Franz law: $\kappa_e(T) = L_0 T / \rho(T)$, where L_0 denotes

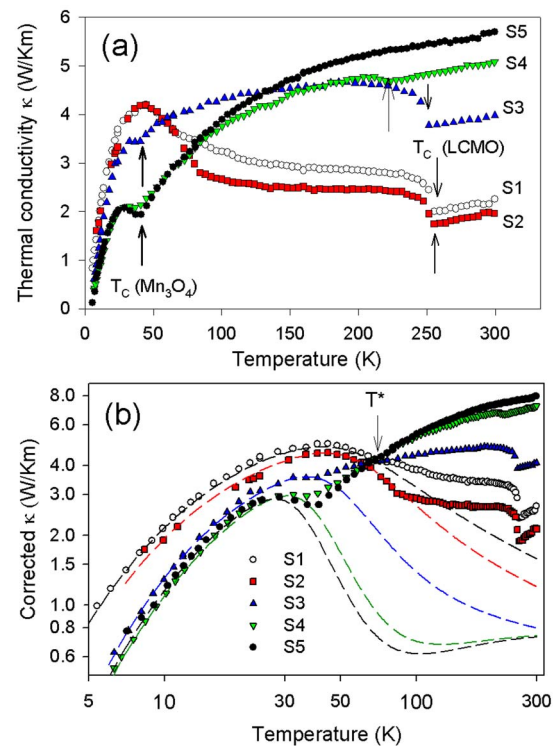


FIG. 2. (Color online) (a) Temperature dependence of the thermal conductivity of LCMO (S1), Mn_3O_4 (S5), and composites of both phases (S2–S4). The arrows indicate the Curie temperatures of Mn_3O_4 and the LCMO phase. (b) Same data corrected for porosity using the Maxwell model and plotted in a log-log scale. Dashed lines: fit using the Debye model.

TABLE II. Fitting parameters of experimental data for the manganite/oxide composite samples using the Debye model.

Sample	B (s^{-1})	E	P ($s^2 K^{-3}$)	D (s^3)	U ($s K^{-1}$)	a (K)	v_{ph} ($m s^{-1}$)	θ (K)	Λ_b (μm)
S1	2.4×10^8	3.8×10^7	100	2200	3.5×10^5	152	4000	450	17.0
S2	5.6×10^8	2.5×10^7	8 500	2400	8.5×10^5	200	4250	450	7.6
S3	2.4×10^9	5.0×10^5	15 500	2250	4.0×10^6	200	3900	450	1.6
S4	2.2×10^9	9.0×10^7	16 000	2400	3.0×10^7	210	3200	450	1.5
S5	2.2×10^9	7.4×10^7	18 000	2400	3.5×10^7	190	3200	450	1.5

the Lorenz number ($L_0=2.44 \times 10^{-8} W \Omega K^{-2}$) and $\rho(T)$ is the electrical resistivity. The resulting $\kappa_c(T)$ values are smaller than 1% of the total thermal conductivity and will be neglected. Due to the same statistics for magnons and phonons, κ_{magn} cannot be separated easily from the total thermal conductivity, unless high magnetic fields are used.^{23,24} In the case of a linear dispersion law of magnons, however, their final contribution to the thermal conductivity is described by the Debye integral²⁵ as in the case of phonons, i.e.,

$$\kappa = GT^3 \int_0^{\Theta/T} \frac{x^4}{\tau^{-1} \sinh^2(x/2)} dx, \quad (2)$$

where $x = \hbar\omega/k_B T$ ($\hbar\omega$ is the phonon energy), G is a constant, θ is the Debye temperature, and τ^{-1} is the sum of inverse relaxation times for various phonon scattering processes: $\tau^{-1} = \sum \tau_i^{-1}$, where $\tau_i = \tau_b, \tau_e, \tau_d, \tau_N,$ and τ_U denote, respectively, the relaxation times for phonon scatterings on grain boundaries, on conduction electrons, and on defects, and for normal scattering and umklapp scattering. Simple dependences of the relaxation times on ω and T are assumed, namely, $\tau_b^{-1} = B$, $\tau_e^{-1} = E\omega$, $\tau_d^{-1} = D\omega^4$, $\tau_{ph}^{-1} = P(\omega T)^3$, and $\tau_U^{-1} = U\omega^2 T \exp[-a/T]$, where $B, E, D, P, U,$ and a are constants.²⁵

In Fig. 2(b) we illustrate how Eq. (2) fits our experimental data (dashed curves). The agreement with the Debye model is excellent in the temperature range of 5–100 K for samples S1 and S2 and in the range of 5–50 K for S3–S5. The constants $B, E, P, D,$ and U , obtained from the fitting procedure, are shown in Table II. Although a wide interval of magnitudes was allowed for the sound velocity v_{ph} (confined in the interval of 1000–5000 m/s) and the Debye temperature θ (350–450 K), the final values of these parameters are surprisingly close to each other and are in good agreement with literature data.^{26,27} The mean free paths of the phonons scattered by grain boundaries (Λ_b) were determined from τ_b and v_{ph} ($\Lambda_b = \tau_b v_{ph}$) and are listed in Table II. Although all samples are characterized by similar average grain sizes (1–10 μm), the Λ_b values are found to decrease with increasing Mn_3O_4 content. This feature can be qualitatively explained by observing micrographs of fractured samples (Fig. 1). In sample S1 [Fig. 1(a)], the grains are so well connected that grain boundaries cannot be distinguished. This correlates the fact that the mean free path ($\sim 17 \mu m$) of phonons scattered by boundaries exceeds the mean grain size. In sample S3, the large number of interfaces between ellipsoidal grains is clearly visible [Fig. 1(b)]. The phonons are thus effectively scattered by grain boundaries and the Λ_b

value matches the grain size (1–2 μm). In sample S5, the Λ_b value ($\sim 1.5 \mu m$) is smaller than the grain size (5–10 μm), which suggests that twins in Mn_3O_4 grains may act as scattering interfaces for phonons. These characteristics may indicate that the relevant length scale determining the scattering of phonons on “interfaces” is not necessarily the size of the grains but strongly depends on the grain structure and connectivity.

The prospect of spin injection and other devices depends strongly on the development of reliable technology for high-quality composite structures of CMR, dielectric, and also high-temperature superconducting materials. The electric and magnetic properties of the systems are significantly influenced by growth peculiarities such as interface smoothness, atomic interdiffusion, and phase distribution. It has been indicated above that porosity is to be considered, and the more so if thermal properties are to be considered or are of technical interest.

V. FINAL REMARKS

The thermal conductivity data $\kappa(T)$ measured on bulk, dense LCMO/ Mn_3O_4 composite samples containing various proportions of both phases allowed us to highlight two significant features. First, in the temperature range where the thermal conductivity of LCMO is close to that of Mn_3O_4 , the thermal conductivities of all samples are the same, as expected in an ideal composite, provided that an appropriate porosity correction is applied. This fact emphasizes the importance of properly estimating the porosity in such composites. Second, a curve fit of the low-temperature part of $\kappa(T)$ using the Debye model suggests that the mean free path of phonons scattered on “boundaries” is on the order of the grain size, but is also influenced by the grain arrangement and by the presence of twins.

ACKNOWLEDGMENTS

This work was partially funded by a collaboration program between the FRS-FNRS (Belgium) and the PAN (Poland). We thank the ULg and the FRS-FNRS for cryofluid and equipment grants.

¹P. K. Siwach, H. K. Singh, and O. Srivastava, *J. Phys.: Condens. Matter* **20**, 273201 (2008).

²J. M. D. Coey, M. Viret, and S. von Molnar, *Adv. Phys.* **48**, 167 (1999).

³M. B. Salamon and M. Jaime, *Rev. Mod. Phys.* **73**, 583 (2001).

⁴M. Ziese, *Rep. Prog. Phys.* **65**, 143 (2002).

⁵B. Vertruyen, R. Cloots, A. Rulmont, G. Dhalenne, M. Ausloos, and Ph. Vanderbemden, *J. Appl. Phys.* **90**, 5692 (2001).

⁶N. D. Mathur, G. Burnell, S. P. Isaac, T. J. Jackson, B.-S. Teo, J. L.

- MacManus-Driscoll, L. F. Cohen, J. E. Evetts, and M. G. Blamire, *Nature (London)* **387**, 266 (1997).
- ⁷S. Valencia, O. Castaño, J. Fontcuberta, B. Martínez, and Ll. Balcells, *J. Appl. Phys.* **94**, 2524 (2003).
- ⁸D. K. Petrov, L. Krusin-Elbaum, J. Z. Sun, C. Feild, and P. R. Duncombe, *Appl. Phys. Lett.* **75**, 995 (1999).
- ⁹B. Vertruyen, J.-F. Fagnard, Ph. Vanderbemden, M. Ausloos, A. Rulmont, and R. Cloots, *J. Eur. Ceram. Soc.* **27**, 3923 (2007).
- ¹⁰B. Vertruyen, R. Cloots, M. Ausloos, J.-F. Fagnard, and Ph. Vanderbemden, *Phys. Rev. B* **75**, 165112 (2007).
- ¹¹B. Vertruyen, R. Cloots, M. Ausloos, J.-F. Fagnard, and Ph. Vanderbemden, *Appl. Phys. Lett.* **91**, 062514 (2007).
- ¹²J. J. Couderc, S. Fritsch, M. Brieu, G. Vanderschaeve, M. Fagot, and A. Rousset, *Philos. Mag. B* **70**, 1077 (1994).
- ¹³A. Jeżowski, J. Mucha, and G. Pompe, *J. Phys. D* **20**, 1500 (1987).
- ¹⁴J. Mucha, S. Dorbolo, H. Bougrine, K. Durczewski, and M. Ausloos, *Cryogenics* **44**, 145 (2004).
- ¹⁵K. Dwight and N. Menyuk, *Phys. Rev.* **119**, 1470 (1960).
- ¹⁶J. Hejtmanek, Z. Jiráček, S. Krupička, C. Martin, Ch. Simon, A. Maignan, B. Raveau, E. Grivei, and J. P. Issi, *J. Appl. Phys.* **81**, 4975 (1997).
- ¹⁷D. W. Visser, A. P. Ramirez, and M. A. Subramanian, *Phys. Rev. Lett.* **78**, 3947 (1997).
- ¹⁸J. L. Cohn, *J. Supercond. Novel Magn.* **13**, 291 (2000).
- ¹⁹J. C. A. Maxwell, *Treatise on Electricity and Magnetism* (Dover, New York, 1954).
- ²⁰R. Pal, *Composites, Part A* **39**, 718 (2008).
- ²¹J. E. Parrott and A. D. Stuckes, *Thermal Conductivity of Solids* (Pion, London, 1975).
- ²²R. Berman, *Thermal Conduction in Solids* (Clarendon, Oxford, 1976).
- ²³D. Varshney and N. Kaurav, *J. Low Temp. Phys.* **147**, 7 (2007).
- ²⁴I. A. Smirnov and V. S. Oskotski, in *Handbook on the Physics and Chemistry of Rare Earths*, edited by K. A. Gschneider and L. Eyring (North-Holland, Amsterdam, 1993), Vol. 16.
- ²⁵J. Callaway, *Phys. Rev.* **113**, 1046 (1959).
- ²⁶H. Fujishiro, T. Fukase, and M. Ikebe, *J. Phys. Soc. Jpn.* **67**, 2582 (1998).
- ²⁷M. Battabyal and T. K. Dey, *Physica B* **373**, 46 (2006).